Impact of Dispersion on Gel Placement for Profile Control

R.S. Seright, SPE, New Mexico Petroleum Recovery Research Center

Summary. A key issue in gel technology is how to place gels in thief zones without damaging oil-productive zones. This study explores the influence of diffusion, dispersion, and viscous fingering during placement of gels to modify injection profiles. These phenomena usually will not eliminate the need for zone isolation during gel placement in unfractured injection wells. During gel placement in parallel laboratory corefloods, diffusion and dispersion can cause one to conclude erroneously that zone isolation is not needed in field applications. Gel treatments are more likely to improve sweep efficiency in wells where fractures are the source of the channeling problem.

Introduction

At the peak of activity, 35% of the EOR projects in the U.S. were polymer projects.[1] About 60% of these polymer projects were gel treatments rather than traditional polymer floods.[2] The objective of gel treatments is to block fractures or watered-out, high-permeability zones so that subsequently injected fluids are more likely to enter and to displace oil from other strata. Many gel projects have been very successful, but unfortunately, others have been technical failures. One study revealed that <45% of near-wellbore gel treatments were successful.[3] The sporadic success rate for gel treatments may be partly a result of the way the gels were placed in the reservoir. In most cases when gelling agents were injected, zones were not isolated, so the chemicals had access to all open intervals. Much of the gel formulation entered fractures and/or high-permeability streaks. However, some of this fluid penetrated into strata that one does not want to plug. Therefore, a key issue in gel technology is how to place gels in fractures or thief zones without damaging oil-productive zones.

Two recent studies[4,5] examined how injection-flow profiles are modified by unrestricted injection of Newtonian and non-Newtonian gelling agents. These studies found the following.

1. Zone isolation is much more likely to be needed during placement of gels in unfractured wells than in fractured wells.
2. Productive zones in unfractured wells can be seriously damaged if zones are not isolated during gel placement.
3. If zones are not isolated during gel placement, the minimum penetration into unfractured, low-permeability zones can be achieved by use of a water-like gelling agent (having a resistance factor of unity).
4. Compared with water-like gelling agents, the non-Newtonian rheology of existing polymeric gelling agents will not reduce the need for zone isolation during gel placement.

This study explores the influence of diffusion, dispersion, and viscous instabilities during placement of gels to modify injection profiles. In particular, these phenomena are examined to determine whether they can be exploited to optimize gel placement.

Several terms should be defined for the reader's benefit. The terms "gelant" and "gelling agent" refer to the liquid formulation before gelation. Resistance factor, F_r, is defined as water mobility divided by gelant mobility, and is equivalent to the effective viscosity of the gelant in porous media relative to that of water. Residual resistance factor, F_{rr}, is defined as water mobility in the absence of gel divided by water mobility in the presence of gel. Residual resistance factor is a measure of the permeability reduction caused by gel.

Gelant Penetration in Oil-Productive Strata

A common misconception in the application of gel treatments is that injected gelling agents will exclusively enter high-permeability, watered-out channels without penetrating to any significant extent into less-permeable, oil-bearing strata. Straightforward application of the Darcy equation reveals that gelling agents can penetrate to a significant degree into all open intervals.[4,5] For example, if a gelant penetrates 50 ft [15.2 m] radially from an injection well into the most-permeable layer of a multilayer reservoir, then the gelant can propagate at least 5 ft [1.5 m] radially into a zone that is 100 times less permeable, as **Fig. 1** shows. Fig. 1 plots the depth of penetration (final radius minus wellbore radius) of gelant into a less-permeable zone (Layer 2, k_2) when the gelant reaches 50 ft [15.2 m] into the most-permeable zone (Layer 1, k_1). (The wellbore radius is 0.5 ft [0.15 m], and all layers have the same porosity.) This information is shown for two Newtonian fluids ($F_r=1$ and $F_r=100$) and two non-Newtonian fluids. The non-Newtonian fluids included a xanthan solution and a partially hydrolyzed polyacrylamide (HPAM) solution. (Flow properties of the non-Newtonian fluids are described in Ref. 5.) Note that for a given permeability ratio, the three viscous fluids penetrate to a greater depth in the less-permeable layer than does the water-like fluid ($F_r=1$).

For the calculations represented in Fig. 1, no crossflow occurs between layers. If crossflow can occur between layers or flow paths in a reservoir, viscous gelants will penetrate into low-permeability layers to a greater extent. In fact, under some circumstances (if the gelant/water mobility ratio is less than the permeability contrast between adjacent layers), the depth of penetration of gelant in a low-permeability layer can be almost the same as that in an adjacent high-permeability layer.[6,7] Thus, if crossflow can occur, viscous gelants can damage oil-productive zones to a greater extent than they can if crossflow is not possible.

In preparing Fig. 1, diffusion, dispersion, chemical retention, and inaccessible PV effects were neglected. The impact of chemical retention and inaccessible PV on these calculations has been described previously.[4,5] The role of diffusion and dispersion is discussed in this paper.

Dilution by Diffusion

In concept, diffusion and dispersion could dilute gelling agents enough to prevent gelation in less-permeable, oil-productive zones while still allowing a gel plug to form in watered-out, high-permeability streaks.[8] Whether or not a chemical bank can be diluted enough by diffusion to prevent gelation depends on at least four factors: the size of the chemical bank, the diffusion coefficient, the gelation time, and the extent of dilution required to prevent gelation.

Diffusion coefficients are typically on the order of 1.5×10^{-6} in.^{2}/sec [10^{-5} cm^2/s] for low-molecular-weight chemicals in water.[9] These chemicals include such gelling agents as acrylamide monomer, phenol, and formaldehyde. Diffusion coefficients are typically on the order of 1.5×10^{-9} in.^{2}/sec [10^{-8} cm^2/s] for high-molecular-weight polymeric gelling agents, such as polyacrylamide or xanthan.[10] For low-molecular-weight species in a viscous polymer solution (e.g., $Cr_2O_7^{2-}$ in water with 2,000 ppm polyacrylamide), the diffusion coefficient should have some intermediate value that varies inversely with the solution viscosity.[9] The relationship between the apparent diffusion coefficient, D, in porous media and the molecular binary diffusion coefficient, D_o, has been described by

$$D=D_o/(R\phi), \quad \ldots\ldots\ldots\ldots\ldots\ldots\ldots\ldots\ldots\ldots\ldots\ldots (1)$$

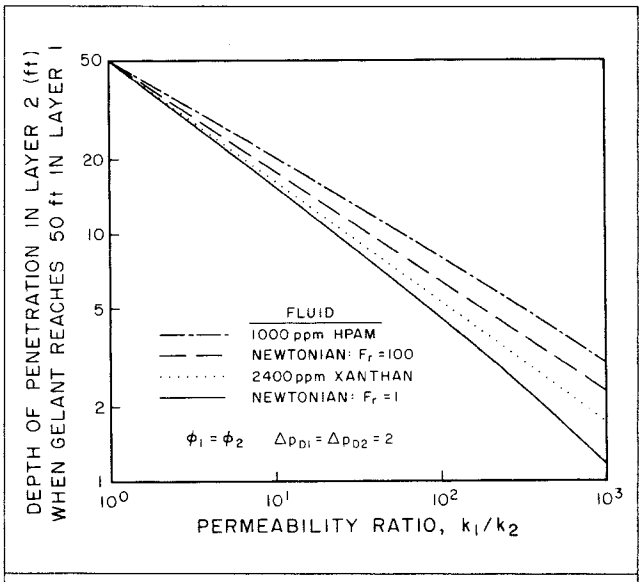

Fig. 1—Relative penetration of fluids in an unfractured injection well with multiple noncommunicating layers.

where R=formation electrical resistivity and ϕ=porosity. Apparent diffusion coefficients in porous media are commonly 20 to 40% less than molecular diffusion coefficients.[11]

Gelation times range from a few minutes to several days for most formulations that have been considered for near-wellbore gel treatments. In general, the gelation time decreases with increasing concentrations of the gelling agents.[12,13] Also, some minimum concentration of the proper reactants must be present for gelation to occur. In most field applications of gel treatments, the concentrations of reactants that are injected are well above the minimum levels required for gelation. Thus, significant dilution (often by a factor of two or more) is required to prevent gelation.

For much of this study, we assume that the gelation reaction is stopped by only a 10% dilution of the reactants. Thus, the reader should bear in mind that the reductions in gel-bank size owing to dilution by diffusion and/or dispersion that are forecast will be overly optimistic. By overestimating the effect of diffusion and dispersion in this analysis, we increase confidence in a major conclusion from this study; i.e., in field applications, diffusion and dispersion will not usually cause enough dilution to prevent gelation in the less-permeable zones.

In field applications of gel treatments, wells are commonly shut in for some time after injection of the gelling agent to allow the gel to form. During the time before gelation, diffusion acts to dilute the chemical banks (see **Fig. 2A**). The size of the mixing zone, L_m, created by diffusion alone (no dispersion) during this time can be approximated with

$$L_m = 3.62\sqrt{Dt_g}, \quad \ldots\ldots\ldots\ldots\ldots\ldots\ldots\ldots\ldots\ldots (2)$$

where t_g=gelation time. The mixing zone given by Eq. 2 extends from the point where the gelling agent has been diluted to 90% of the original concentration to the point where the gelling agent has been diluted to 10% of the original concentration.[11] **Fig. 2B** illustrates a typical concentration profile that results when diffusion or dispersion smears an interface that was originally sharp, as well as the size of the mixing zone given by Eq. 2.

If the gelation reaction is stopped by a 10% dilution of the reactants, then diffusion will reduce the gel-bank size by the distance $L_m/2$. **Fig. 3** provides values of $L_m/2$ as a function of time and diffusion coefficient. A key point illustrated by Fig. 3 is that diffusion will not create a large mixing zone in the period associated with typical gelation times. Even for relatively large diffusion coefficients (1.5×10^{-6} in.^{2}/sec [10^{-5} cm^2/s]), $L_m/2$ is only about 0.2 ft [6 cm] after 10 days. Considering the depths of penetration for gelling agents in typical field applications (see Fig. 1), diffusion is not likely to have a significant impact on a field scale.

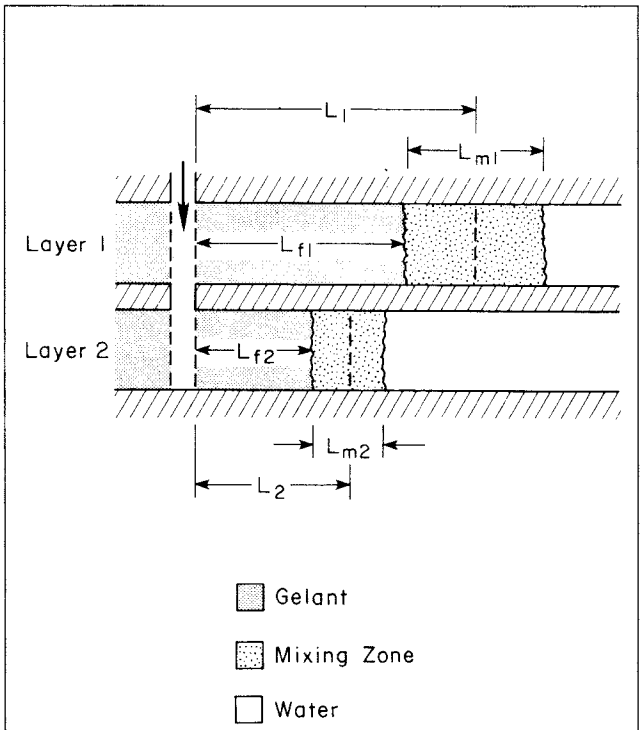

Fig. 2A—Gel-bank lengths without diffusion or dispersion, L_1 and L_2, vs. with diffusion or dispersion, L_{f1} and L_{f2}.

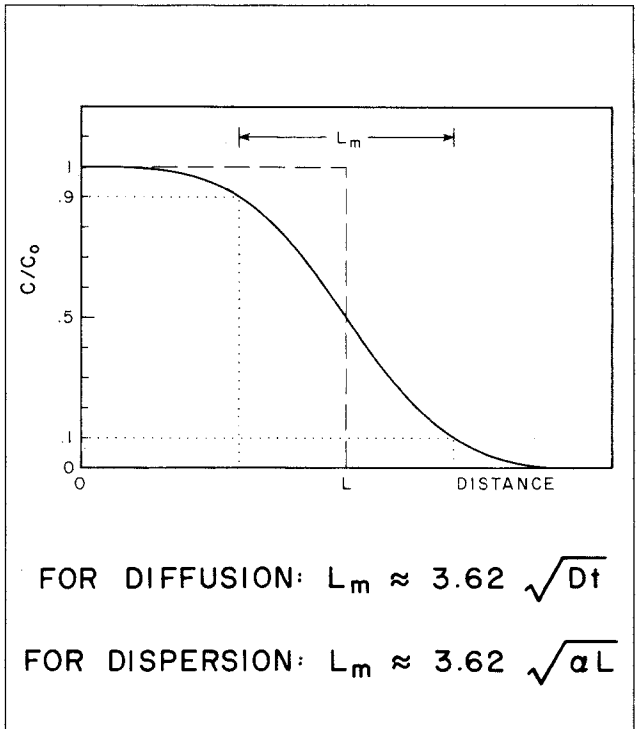

Fig. 2B—Concentration profile at the interface between the water and gelling-agent banks.

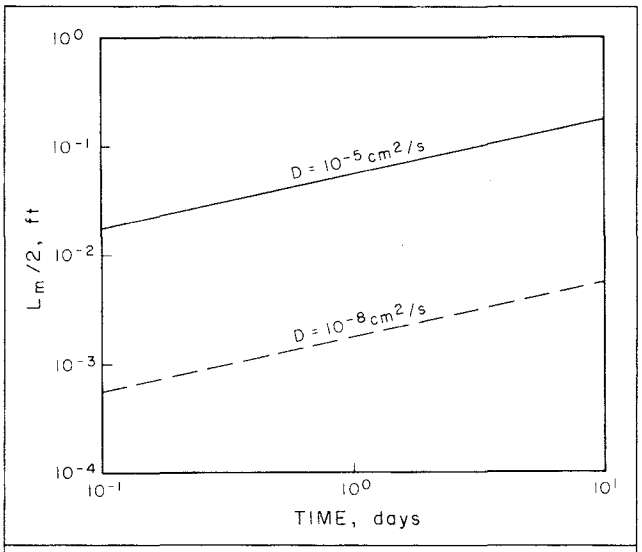

Fig. 3—Length of mixing zone caused by diffusion.

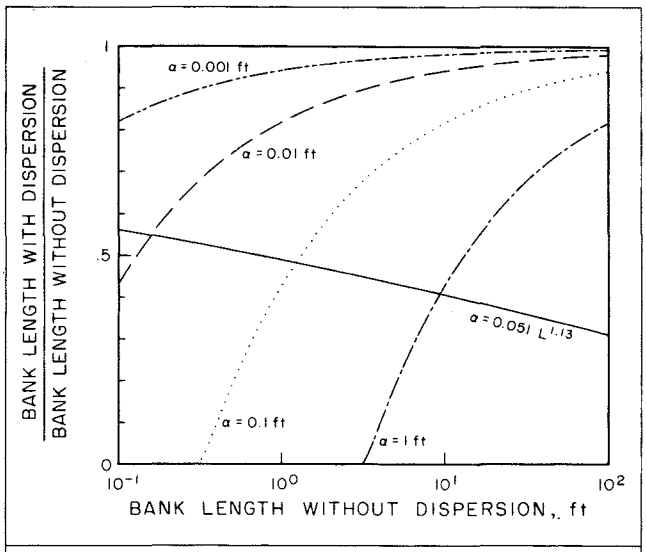

Fig. 4—Effect of dispersion on bank size.

In contrast, diffusion can significantly affect results from parallel laboratory corefloods. Consider injection of a 1-cp [1-mPa·s] gelling agent to displace water from two 1-ft [0.3-m] -long cores that are being flooded in parallel. Assume that one core is 10 times more permeable than the other and that both cores have the same porosity. When the gelling agent reaches the outlet of the most-permeable core, the gelling agent will have penetrated 0.1 ft [0.03 m] into the less-permeable core. Over the course of 1 day, most of the gelling agent in the less-permeable core could be diluted if the diffusion coefficient is 1.5×10^{-6} in.^{2}/sec [10^{-5} cm^2/s].

Dilution by Dispersion

During injection of a gelant to displace water miscibly, both diffusion and dispersion will occur. While diffusion is the transport of mass because of spatial concentration differences, dispersion is mixing caused by variations in the velocity within each flow channel and from one channel to another.[14] In flow through reservoirs, dispersion usually is much more important than diffusion.[14]

The size of the mixing zone (again, between the 90 and 10% concentration levels) created by dispersion can be estimated with

$$L_m = 3.62\sqrt{\alpha L}, \quad \ldots\ldots (3)$$

where α=dispersivity of the porous medium and L=distance traveled by the fluid front. Laboratory values for α commonly are in the range from 0.001 to 0.05 ft [0.0003 to 0.015 m].[14,15] However, field dispersivity values are usually significantly greater than laboratory values because of the greater heterogeneity experienced on the larger scale.[14,16] Using more than 60 dispersivity values from both field and laboratory measurements, Arya *et al.*[14] noted that the following relation correlates dispersivity values over a wide range of length scales (although there is considerable scatter in the data):

$$\alpha = 0.044\ L^{1.13}, \quad \ldots\ldots (4a)$$

if α and L are expressed in meters, and

$$\alpha = 0.051\ L^{1.13}, \quad \ldots\ldots (4b)$$

if α and L are expressed in feet.

The above information can be used to estimate reductions in the size of a gel bank resulting from dilution by dispersion. **Fig. 4** shows these estimates as functions of dispersivity and original bank size, L. The size of the gel bank after dispersion, L_f, relative to the original bank size was approximated with

$$L_f/L = [1 - L_m/(2L)]. \quad \ldots\ldots (5)$$

Four constant-dispersivity cases are shown. These cases indicate that the smallest chemical banks should experience the greatest dilution by dispersion. However, very high near-wellbore dispersivity values (~1 ft [~0.3 m]) are required to prevent gelation during typical field gel treatments (compare Fig. 4 with Fig. 1).

TABLE 1—MIXING-ZONE LIMITS

Concentration Limits of Mixing Zone (%)	Coefficient in Eqs. 2 and 3
95 to 5	4.65
90 to 10	3.62
80 to 20	2.38
70 to 30	1.48
60 to 40	0.72
50 to 50	0.00

In contrast to the calculations made with constant dispersivity values, the Arya correlation (Eq. 4b) predicts that the relative reduction in bank size will be fairly insensitive to the length of the original (undiluted) gel bank. In fact, the correlation actually suggests that dispersion has a slightly greater effect as bank size increases (see Fig. 4). Therefore, if the Arya correlation applies, dispersion will not inhibit gel formation in low-permeability zones to a greater extent than in high-permeability zones.

For a given length scale, different strata may exhibit different dispersivities. Thus, in concept, one could exploit a situation where the dispersivity was much higher in the less-permeable layers than in the most-permeable layers. However, close examination of Fig. 4 suggests that the dispersivity contrast must be very large to be exploitable.

Figs. 3 and 4 are most applicable for diffusion and dispersion in a linear geometry. The relative reduction in chemical-bank size will be less in a radial geometry than in a linear geometry.[17]

In the discussion to this point, gelation is assumed to be prevented by a 10% reduction of the original concentration of gelling agent. As mentioned earlier, the effect of diffusion and dispersion is generally overestimated with this assumption. Other values may be used for the concentration below which gelation does not occur. In general, if the minimum concentration for gelation is >50% of the original concentration, then diffusion and dispersion will reduce the size of the gel bank in a given zone. However, if the minimum concentration for gelation is <50% of the original concentration, then the gel bank will be increased in size by the action of diffusion and dispersion. (Of course, the final gel strength in the mixing zone may not be as great as that in the undiluted portion of the gel bank.) To approximate a mixing-zone size, L_m, with limits other than the 90 and 10% concentration levels, the coefficient 3.62 in Eqs. 2 and 3 can be replaced by the appropriate value from **Table 1**. These

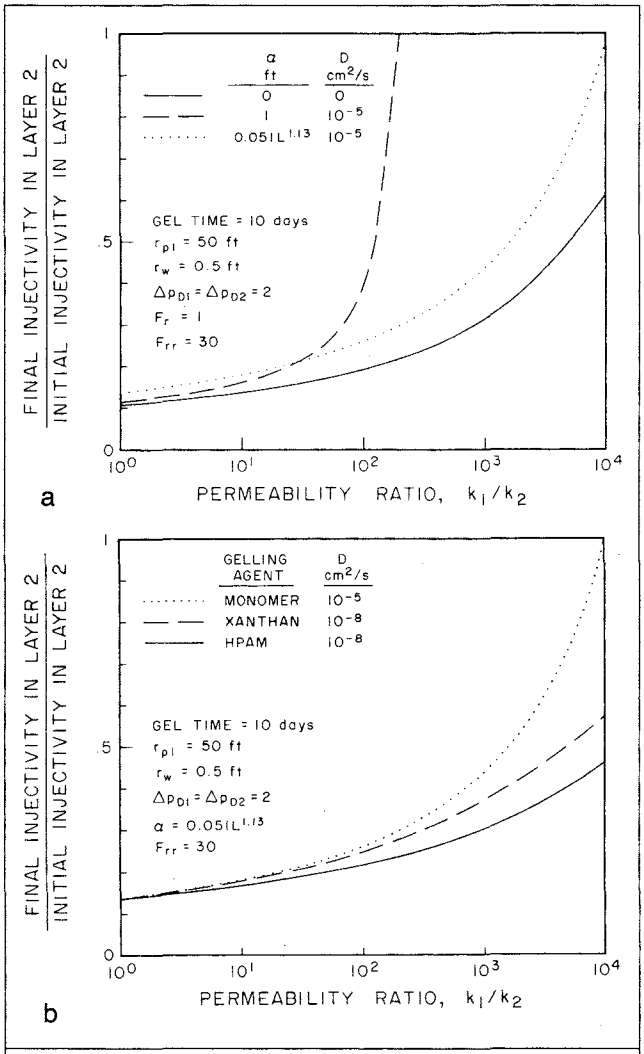

Fig. 5—Reduction of water injectivity after gel placement in unfractured injection wells.

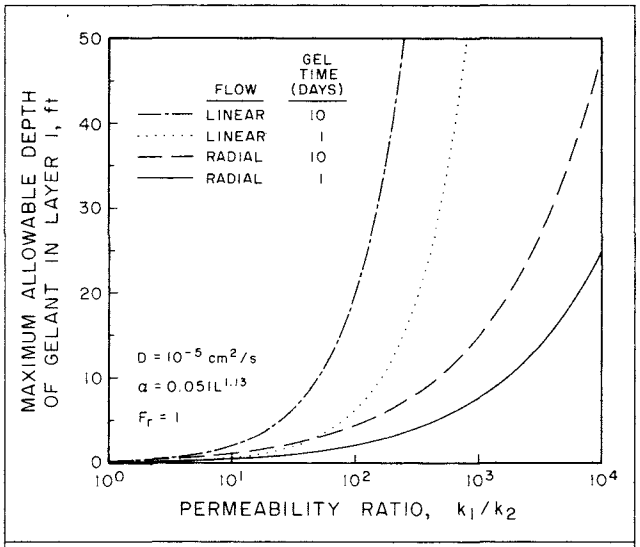

Fig. 6—Exploitation of diffusion and dispersion to prevent gelation in Layer 2.

approximations are valid only for diffusion or dispersion in a 1D, semi-infinite medium where the concentration gradient is described by the standard error-function solution.[11] More sophisticated methods[18,19] may be more appropriate for predicting concentrations in the mixing zone in some cases.

The objective of conventional gel treatments is to reduce injectivity in high-permeability, watered-out zones while maintaining injectivity in less-permeable, oil-productive zones. **Figs. 5a and 5b** compare injectivity behavior for gel placement in an unfractured (radial flow) injection well where the gelling agent is allowed to penetrate 50 ft [15.2 m] into the most-permeable layer (Layer 1). The gelling agent penetrates into a less-permeable layer (Layer 2) to a radius determined by the Darcy equation and the rheology of the gelling agent.[4,5] (The particular reservoir model used here corresponds to the $\Delta p_{D1}=2$, $\Delta p_{D2}=2$ unfractured injection well in Refs. 4 and 5.) Diffusion and dispersion are allowed to the extents calculated with Eqs. 2 and 3, respectively. Various diffusion coefficients and dispersivity values were examined, as indicated on Figs. 5a and 5b. To maximize dilution by diffusion, the gelation time was assumed to be 10 days. Wherever gel forms, the permeability to water is assumed to be reduced by a factor of 30 ($F_{rr}=30$). The Carreau rheological model for a 2,400-ppm xanthan solution was used to generate the xanthan curve. To generate the HPAM curve, the Heemskerk dual power-law model for a 1,000-ppm polyacrylamide solution was used. Both rheological models are described and illustrated in Ref. 5. For the monomer curves, the resistance factor for the gelling agent had a value of unity.

Figs. 5a and 5b indicate that for conventional gel treatments in unfractured injection wells, the injectivity (of water after the gel treatment) will be reduced to about the same extent in all layers that have permeabilities greater than 0.01 times that of the most-permeable layer. If we assume an extremely large near-wellbore dispersivity ($\alpha=1$ ft [0.3 m]), dilution by diffusion and dispersion could eliminate the need for zone isolation during gel placement if the permeability contrast (k_1/k_2) is greater than 100:1. However, with more realistic dispersion behavior (i.e., the Arya correlation), diffusion and dispersion will not have a significant impact for permeability contrasts of less than 1,000:1.

If diffusion and dispersion are to be exploited to eliminate the need for zone isolation during gel placement, then much smaller gelant banks must be used. **Fig. 6** provides a means to estimate the maximum allowable depth of penetration of gelant in the most-permeable layer (Layer 1) for diffusion and dispersion to prevent gelation in a given less-permeable layer (Layer 2) for both linear geometries (e.g., fractured injection wells) and radial geometries (e.g., unfractured injection wells). The reader should note that Fig. 6 was generated by assuming that a monomeric gelant was used ($D=1.5\times10^{-6}$ in.^{2}/sec [10^{-5} cm^2/s] and $F_r=1$) and that only 10% dilution is required to prevent gelation. Thus, Fig. 6 tends to overestimate the effect of diffusion and dispersion, especially for polymeric gelants.

Diffusion and dispersion during gel placement in parallel laboratory corefloods can cause one to conclude erroneously that zone isolation is not needed during gel placement in field projects. **Fig. 7** shows the fraction of original injectivity retained in cores after gel placement in 1-ft [0.3-m] -long parallel linear corefloods. For core permeability ratios of 10:1 or greater, the gelling agent could be diluted sufficiently to prevent gelation in the less-permeable core.

Effect of a Water Postflush on Water-Like Gelant Banks

Additional mixing and thinning of gelant banks can be induced by injecting water to displace gelants away from the wellbore before gelation. The effect of a water postflush will be considered in two parts. In this section, the discussion focuses on displacement of a water-like gelant ($F_r=1$) by water injection. The next section discusses the case where water displaces a viscous gelant.

If water is injected to displace a water-like gelant, the mobility ratio for the displacement is unity. In radial flow, injection of a water postflush will thin the gelant bank, even in the absence of diffusion and dispersion. This thinning is not large, however, and it occurs to about the same proportion in all zones (**Fig. 8**). The situation represented in Fig. 8 is as follows. First, a water-like gelant is injected into a radial, multilayer reservoir until the gelant propagates to a radius of 50 ft [15.2 m] in the most-permeable layer (Layer 1). (The wellbore radius is 0.5 ft [0.15 m], and all layers have the

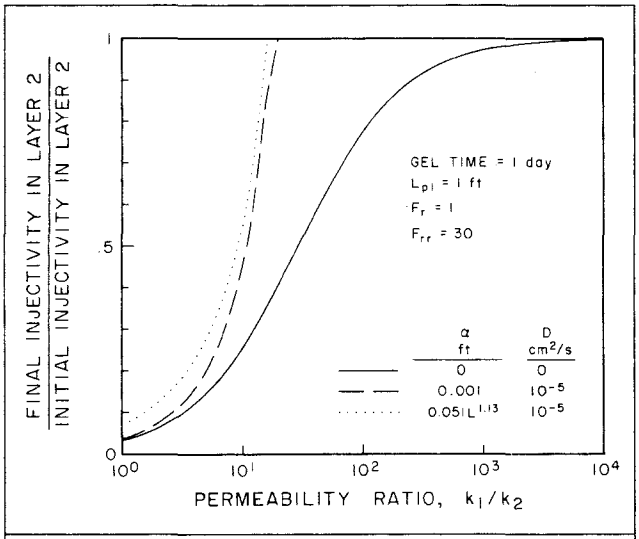

Fig. 7—Reduction of water injectivity after gel placement in parallel linear cores.

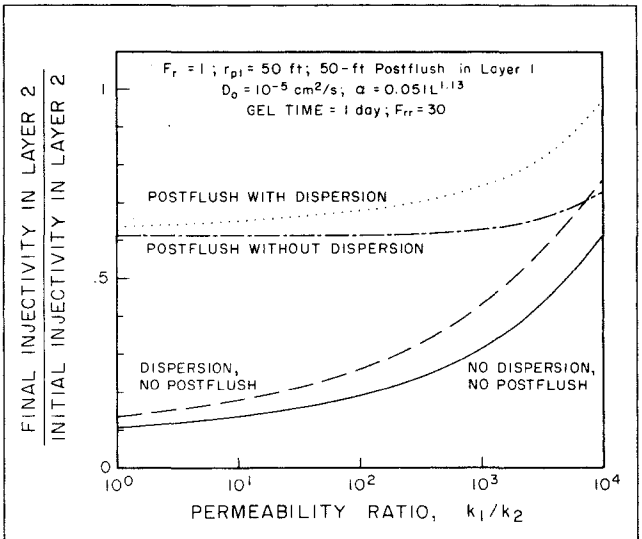

Fig. 9—Effect of water postflush on injectivity.

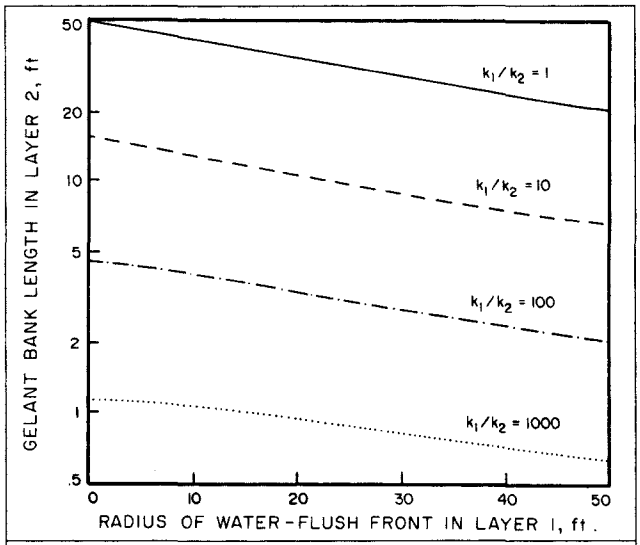

Fig. 8—Thinning of a gelant bank during a water postflush in radial flow.

same porosity.) At this time, the length of the gelant bank (bank radius minus the wellbore radius) will be 49.5, 15.3, 4.5, and 1.2 ft [15.1, 4.7, 1.4, and 0.37 m] in layers that have permeabilities that are 1, 10, 100, and 1,000 times less than that in the most-permeable layer, respectively. After injection of the gelant, water is injected to displace the gelant away from the wellbore. Fig. 8 plots the length of the gelant bank in a given zone (Layer 2, where the permeability ratio, k_1/k_2, is specified in the figure) as a function of the radius of the water postflush in the most-permeable zone. Fig. 8 reveals that a water postflush out to 50 ft [15.2 m] in the most-permeable zone reduces the length of the gelant bank in all zones by roughly a factor of two.

The objective of conventional gel treatments is to reduce injectivity in high-permeability, watered-out zones while maintaining injectivity in less-permeable, oil-productive zones. **Fig. 9** shows the effect of a water postflush on injectivities. Four cases are illustrated. In all four cases, a water-like ($F_r=1$) gelant was allowed to penetrate 50 ft [15.2 m] radially into the most-permeable layer. The gelant penetrated to some lesser radius in a given less-permeable layer. In two cases, dispersion was allowed to occur during fluid injection. The dispersivity was given by Eq. 4b. Diffusion was also allowed to occur at the gelant/water interface (before gelation). The diffusion coefficient was 1.5×10^{-6} in.^{2}/sec [10^{-5} cm^2/s], and the gelation time was 1 day. In the other two cases, no diffusion or dispersion was allowed.

In two cases illustrated in Fig. 9, a water postflush was injected (before gelation) to displace the inner radius of the gelant bank to 50 ft [15.2 m] from the wellbore in the most-permeable layer. Of course, the postflush had a smaller radius in a given less-permeable layer. One case allowed diffusion and dispersion before gelation, while a second case did not. After gelation, the permeability was reduced by a factor of 30 ($F_{rr}=30$) wherever gel formed. Water injectivity in Layer 2 after gelation was fairly insensitive to permeability ratio for k_1/k_2 values between 1 and 100. For the case with no dispersion, water injectivity after gelation increased from 61 to 62% (of original water injectivity) as the permeability ratio increased from 1 to 100. For the case with dispersion (the dotted curve), water injectivity after gelation increased from 64 to 68% (of original water injectivity) as the permeability ratio increased from 1 to 100.

In two other cases in Fig. 9, no water postflush was used. After gelation, the permeability reduction in the gel bank was again equal to 30. For the case with no dispersion (the solid curve), water injectivity after gelation increased from 11 to 18% (of original water injectivity) as the permeability ratio increased from 1 to 100. For the case with dispersion (the dashed curve), water injectivity after gelation increased from 14 to 25% (of original water injectivity) as the permeability ratio increased from 1 to 100.

Several important points should be noted from Fig. 9. First, a water postflush before gelation can significantly increase injectivity in a radial geometry. Unfortunately, injectivity increases by about the same proportion in all zones. Also, diffusion and dispersion can reduce the size of a gel bank during a water postflush. However, the bank size is reduced by about the same proportion in all zones. Thus, a water postflush usually does not help to eliminate the need for zone isolation during gel placement.

Viscous Fingering

Theoretical. A water postflush before gelation tends to form viscous fingers through a viscous gelant. For a multilayer system where gelant has entered all zones, one needs to know in which zone viscous fingers from a water postflush will first break through the gelant bank. The answer to this question will determine whether viscous fingering can be exploited to eliminate the need for zone isolation during gel placement. The size of the gelant bank is smaller in the less-permeable zones than in the most-permeable zone, so viscous fingers have a shorter distance to travel to achieve breakthrough (see **Fig. 10**). However, the viscous fingers will propagate much more rapidly in the most-permeable zone.

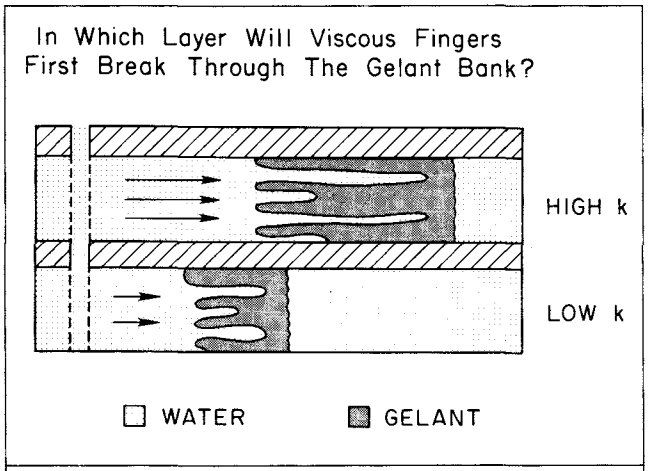

Fig. 10—Viscous fingering.

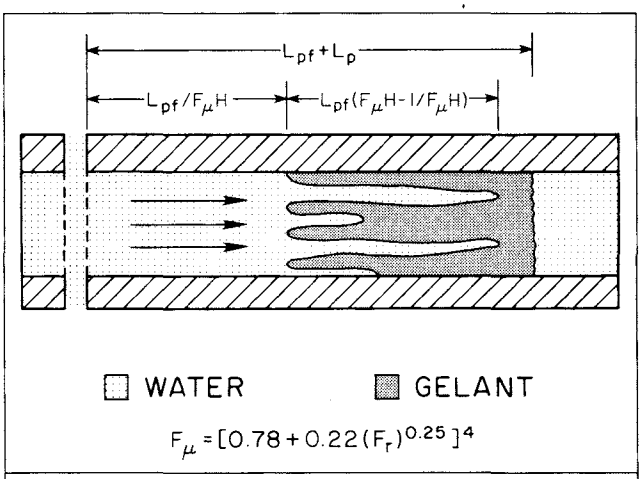

Fig. 11—Quantifying distances during viscous fingering.

Several researchers[20-22] have quantified the growth of viscous fingers during miscible displacements. Koval's[21] analysis appears to be the most widely accepted. According to Koval's analysis, the region between the wellbore and the leading edge of the gelant bank can be divided into three segments (see **Fig. 11**). The first segment extends from the wellbore to the trailing edge of the gelant bank. Water from the postflush is the only mobile fluid in this segment. The length of this segment is $L_{pf}/(F_\mu H)$ for linear flow and $[(r_{pf}^2-r_w^2)/(F_\mu H)+r_w^2]^{0.5}$ for radial flow.[23] Here, L_{pf} and r_{pf}= length and radius, respectively, of the water postflush if the displacement had been piston-like; r_w=wellbore radius; H=heterogeneity factor that ranges from 1 to 5; and F_μ=effective viscosity ratio usually given by the quarter-power mixing rule:

$$F_\mu=[0.78+0.22(F_r)^{0.25}]^4. \quad \ldots\ldots\ldots\ldots\ldots\ldots\ldots\ldots (6)$$

The second segment extends from the trailing edge of the gelant bank to the leading edge of the viscous fingers. This length corresponds to the length of the region of viscous fingers. The length of this segment for linear flow, L_{vf}, is

$$L_{vf}=L_{pf}[F_\mu H-1/(F_\mu H)] \quad \ldots\ldots\ldots\ldots\ldots\ldots\ldots\ldots (7)$$

and for radial flow (r_{vf}) is

$$r_{vf}=[(r_{pf}^2-r_w^2)F_\mu H+r_w^2]^{0.5}-[(r_{pf}^2-r_w^2)/(F_\mu H)+r_w^2]^{0.5}\ldots(8)$$

The third segment extends from the leading edge of the viscous fingers to the leading edge of the gelant bank. Gelant is the only mobile fluid in this segment.

One additional piece of information is required to determine in which zone the viscous fingers will first break through: the effective viscosity, or resistance factor, of the region of viscous fingers. The maximum and minimum possible values for this resistance factor can readily be identified. The maximum value will be the resistance factor of the undiluted gelant, while the minimum value will be the resistance factor of water (with a value equal to unity). The effective viscosity for the region of viscous fingers is often assumed to be given by the quarter-power mixing rule[21-25] (Eq. 6). This rule is most applicable for displacement of a viscous Newtonian fluid by another Newtonian fluid. Stoneberger and Claridge[26] propose Eq. 9 for unstable displacements when pseudoplastic (shear-thinning) fluids are used:

$$F_{\mu p}=[0.50+0.50(F_r)^{0.25}]^4. \quad \ldots\ldots\ldots\ldots\ldots\ldots\ldots\ldots (9)$$

Figs. 12 and 13 address viscous fingering from a water postflush in radial flow. For these figures, a viscous gelant is injected to a radius of 50 ft [15.2 m] in the most-permeable layer (Layer 1). During this time, the gelant penetrates some lesser distance in a given less-permeable layer (Layer 2). Then, before gelation, water is injected to displace the gelant. In Fig. 12, the resistance factor of the undiluted gelant, F_r, is 10. Four different values are considered for the average resistance factor of fluid in the zone of viscous fingers, F_m. The cases where $F_m=1$ and $F_m=F_r$ represent the extremes of possible resistance factors, while $F_m=F_\mu H$ (from the quarter-power mixing rule) provides a best guess. Use of

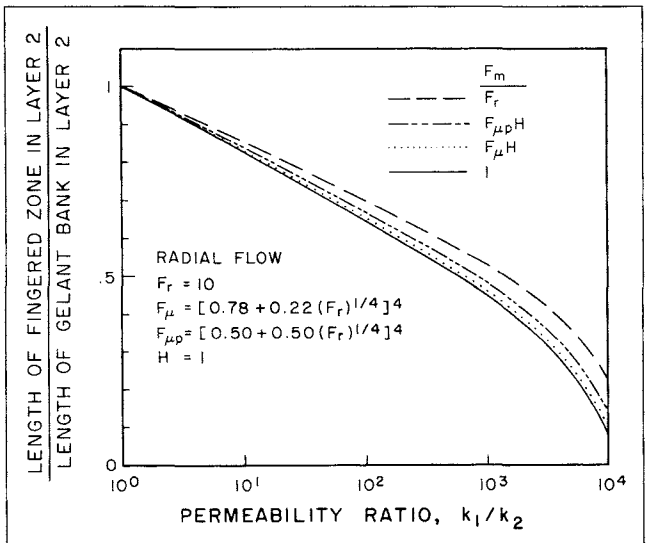

Fig. 12—Sensitivity of finger breakthrough to assumed resistance factor in the fingered zone. Length of fingered zone in Layer 2 when fingers break through in Layer 1.

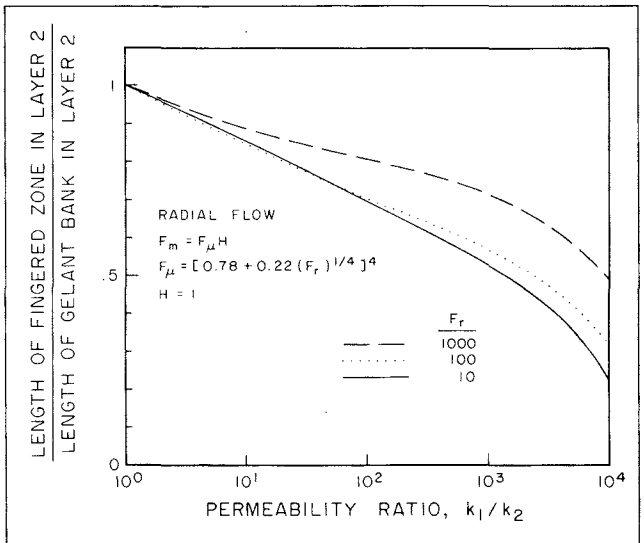

Fig. 13—Sensitivity of finger breakthrough to resistance factor of the viscous fluid. Length of fingered zone in Layer 2 when fingers break through in Layer 1.

$F_m = F_{\mu p} H$ may be applicable for pseudoplastic fluids. For all four cases and for all permeability ratios, viscous fingers are predicted to break through the gelant bank in Layer 1 before breaking through the bank in Layer 2.

Fig. 13 is similar to Fig. 12 except that $F_m = F_\mu H$ for all cases and the resistance factor of the undiluted gelant varies from 10 to 1,000. Again, for all cases and for all permeability ratios, viscous fingers are predicted to break through the gelant bank in the most-permeable layer before breaking through the bank in a given less-permeable layer. Note that for all but the most extreme permeability ratios, however, the fingered zone in the less-permeable layer extends most of the distance through the gelant bank.

Koval's theory has been used widely as a means of quantifying the growth of viscous fingers.[25] On the surface, our use of Koval's theory appears to provide exact predictions. When these predictions are interpreted, however, one must consider the statistical nature of viscous fingering. Within a given layer, there is a random element in where fingers will form and how rapidly a given finger will grow.[25] Thus, Figs. 12 and 13 must be viewed as predictions of what will occur after averaging many trials. On average, Fig. 13 predicts that when viscous fingers break through the bank in Layer 1, the fingers typically will have traversed 60 to 100% of the bank in Layer 2. Alternatively, Fig. 13 predicts that viscous fingers will break through in Layer 1 somewhat more often than in Layer 2.

A similar analysis may be applied for linear flow.[17] That analysis predicts that viscous fingers will break through the gelant bank in a given less-permeable layer at about the same time as in the most-permeable layer. The differences from the radial predictions occur because the gelant-bank length in linear flow does not decrease with distance as it is pushed away from the injection face by the postflush. In radial flow, the gelant-bank length decreases as it moves away from the injection well.

In Figs. 12 and 13, the Koval heterogeneity factor, H, was assumed to have a value of unity in each layer. We have examined the effect of H on the predictions and have found that the results are fairly insensitive to the choice of heterogeneity factor (for H values ranging from one to five).[17]

Note that Figs. 1, 5, 6, 8, 9, and 13 can be applied to reservoirs with many layers. For example, consider a reservoir that has four noncommunicating layers with permeabilities of 10,000, 1,000, 100, and 10 md, respectively. Assume that all layers have the same porosity and that flow is radial. Consider what would happen if a 10-cp [10-mPa·s] fluid were injected to displace 1-cp [1-mPa·s] water. When the viscous fluid reached a radius of 50 ft [15.2 m] from the wellbore in the 10,000-md layer, the fluid would have reached radii of 17.9, 6.7, and 2.6 ft [5.5, 2, and 0.8 m] in the 1,000-, 100-, and 10-md layers, respectively. If a water postflush were subsequently injected until viscous fingers broke through the viscous bank in the 10,000-md layer, then Fig. 13 can be used to find how far viscous fingers had propagated in the other layers. At breakthrough in the 10,000-md layer, the fingers are predicted to traverse 85, 70, and 53% of the viscous banks in the 1,000-, 100-, and 10-md layers, respectively.

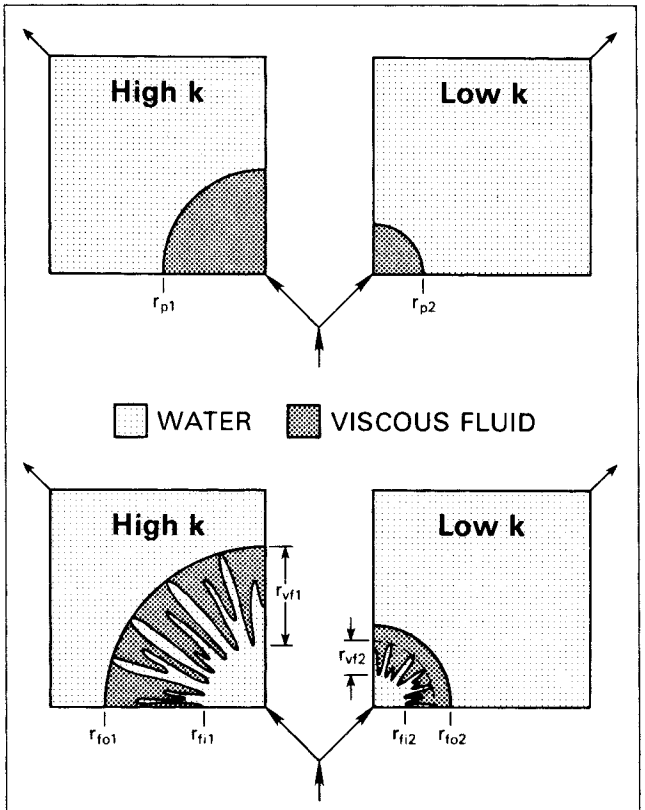

Fig. 14—Important measurements during viscous-fingering experiments.

Experimental Verification. To test the radial-flow predictions, sequential banks of water, viscous fluid, and water were injected into parallel beadpacks. Each beadpack was configured as one-quarter of a five-spot pattern, with one injector and one producer in di-

TABLE 2—SUMMARY OF VISCOUS-FINGERING RESULTS

	Viscous Fluid (Number of Replicates)					
	Ethanediol (10)		2,000-ppm Xanthan (12)		2,000-ppm HPAM (9)	
	High-k Pack	Low-k Pack	High-k Pack	Low-k Pack	High-k Pack	Low-k Pack
Initial radius of viscous fluids, in.	13.9±0.5	5.6±0.7	14.1±0.1	4.6±0.3	13.3±0.5	5.9±0.7
Occasions viscous bank is breached first	7	3	9	3	8	1
Final outer radius of viscous fluid, in.	16.5±1.1	16.2±0.7	15.3±0.4	4.8±0.3	15.6±0.5	6.2±0.7
Final inner radius of viscous fluids, in.	7.8±1.7	3.8±0.8	3.1±0.9	1.7±0.2	4.7±0.6	1.9±0.3
Number of fingers	5±1	18±7	12±3	15±5	7±2	6±2
Length of longest viscous finger, in.	8.0±1.1	1.8±1.0	11.9±0.8	2.7±0.5	10.8±0.4	2.8±1.1
Length of fingered zone relative to length of viscous bank	0.93±0.10	0.71±0.22	0.98±0.03	0.86±0.10	0.99±0.03	0.62±0.16
F_μ						
From fingering data	2.1±0.3	1.6±0.5	5.2±1.7	2.6±0.4	3.3±0.4	2.5±0.9
From Eq. 6	1.9	1.9	2.8	2.7	2.4	2.3
From Eq. 9	4.0	4.0	7.7	7.1	5.8	5.6

agonally opposite corners (see **Fig. 14**). The dimensions of the packs were $22\times22\times0.5$ in. [$56\times56\times1.2$ cm]. The less-permeable pack contained nominally 150-μm glass beads and had a permeability of 13.6 darcies. The more-permeable pack contained nominally 500-μm glass beads and had a permeability of 174 darcies. The porosity of both packs was 0.38, and both packs were initially completely saturated with water. The two packs were flooded in parallel, experiencing the same pressure drop and injection fluid at any given time. The total fluid injection rate (Pack 1 plus Pack 2) was maintained constant at 1440 mL/h.

A viscous water-miscible fluid was injected to reach a radius, r_{p1}, of about 13.8 in. [35 cm] in the most-permeable beadpack. The radius to which the fluid penetrated in the less-permeable pack, r_{p2}, was then noted (see **Table 2**). Fluorescein dye was included with the viscous bank to allow visualization of its boundaries. Three viscous fluids were used: (1) a mixture of 85% ethanediol and 15% water, (2) 2,000 ppm xanthan in water, and (3) 2,000 ppm HPAM in aqueous 0.5% KCl. The ethanediol mixture was Newtonian with a viscosity of 11 cp [11 mPa·s]. The xanthan solution was shear-thinning, exhibited a power-law exponent of 0.36, and had a viscosity of 99 cp [99 mPa·s] at 11 seconds^{-1}. The HPAM solution was also shear-thinning, exhibited a power-law exponent of 0.69, and had a viscosity of 30 cp [30 mPa·s] at 11 seconds^{-1}. Experiments confirmed that polymer adsorption in the beadpacks was negligible. All experiments were conducted at room temperature.

Consistent with the predictions of Refs. 4 and 5, all three viscous agents penetrated to a significant degree into the less-permeable pack. The ratio r_{p2}/r_{p1} was greater than the square root of the permeability ratio, k_2/k_1, in all three cases.

After placement of the viscous banks, water (without fluorescein) was injected until viscous fingers broke through one of the two viscous banks. Injection was then stopped. Note was made of (1) the bank that was first breached by viscous fingers; (2) the final outer radius of the viscous bank in each pack, r_{fo1} and r_{fo2}; (3) the final inner radius of the viscous bank in each pack, r_{fi1} and r_{fi2}; (4) the number of fingers in each bank; (5) the length of the longest finger in each bank, r_{vf1} and r_{vf2}; (6) the length of the longest finger divided by the final length of the viscous bank, and (7) the ratio r_{fo}/r_{fi} for each pack (which should approximately equal $F_\mu H$).

The fingering patterns did not show signs of repeating the same flow paths from run to run, indicating good homogeneity in the beadpacks. For each viscous fluid, the parallel displacement experiments were repeated 9 to 12 times. Fig. 14 illustrates the important measurements made during each experiment. Table 2 lists averages and standard deviation values for the various measurements. Appendix E of Ref. 17 lists results for individual experiments.

For all three viscous fluids, viscous fingers broke through the bank in the high-permeability pack more often than in the low-permeability pack. Regardless of which pack first experienced breakthrough, however, fingers had traversed most of the viscous bank in the other beadpack. These findings are qualitatively in agreement with the theory and have important implications with respect to in-situ dilution and mixing of gelling agents. The results suggest that viscous fingers will facilitate in-situ mixing of fluids to about the same extent in low-permeability zones as in high-permeability zones. This is beneficial if uniform mixing of fluids is desired. However, the results cast doubt on the utility of schemes that rely on nonuniform mixing to optimize gel placement. For example, fingers from a water postflush are not expected to eliminate the need for zone isolation during gel placement (i.e., by breaking through a gelant bank in a low-permeability layer before breaking through in a high-permeability layer). Also, one cannot rely on viscous fingering to promote or to inhibit gelation in one zone to a greater extent than in another zone.

The above observations also have an important implication in traditional polymer floods where crossflow can occur between layers. Researchers[27-29] have suggested that a small bank of a viscous fluid can cause surprisingly high levels of incremental oil recovery if crossflow can occur in a stratified reservoir. They argue that the viscous bank in a high-permeability layer can outrun the bank in less-permeable layers. Then, water behind the viscous bank in the high-permeability layer is forced to cross flow into and to displace oil from the less-permeable layers.

The observations of viscous fingering reported here introduce questions about the validity of this displacement mechanism. The mechanism requires that significant volumes of water from the postflush must cross flow from the high-permeability layer into the low-permeability layer. By implication, this requires that viscous fingers must somehow break through the viscous bank in the low-permeability layer substantially before breakthrough in the high-permeability layer. Our findings raise doubt that this will happen. More work is needed to resolve this issue.

The factor F_μ provides one means to compare theoretical predictions with experimental results. As mentioned earlier, the outer radius of the fingered zone is $[(r_{pf}^2-r_w^2)F_\mu H+r_w^2]^{0.5}$, while the inner radius of the fingered zone is $[(r_{pf}^2-r_w^2)/(F_\mu H)+r_w^2]^{0.5}$. If $H=1$ (which should be the case for our homogeneous beadpacks) and if r_w is negligible, F_μ may be estimated from experimental data. In particular, F_μ is approximately equal to the outer radius of the fingered zone divided by the inner radius of the fingered zone, r_{fo}/r_{fi}. The bottom of Table 2 lists values for F_μ determined in this way from the experimental data. For comparison, Table 2 also lists F_μ values calculated with Eqs. 6 and 9. (The geometrically averaged values for F_r that were used in Eqs. 6 and 9 were 11 and 11 for ethanediol; 30 and 26 for the xanthan solution; and 20 and 19 for the HPAM solution, respectively, in the high- and low-permeability packs.) For all but one of the pack/fluid combinations, Eq. 6 provided a reasonably close match to the experimentally determined value for F_μ. The exception was the xanthan-high-permeability-pack data. Eq. 9 overestimated the experimental F_μ value in all cases.

Note in Table 2 that the final outer radius of the viscous fluid is least for the 2,000-ppm xanthan solution and is greatest for the ethanediol mixture. This is true for both the high- and low-permeability packs and indicates that viscous fingering is most severe for the xanthan solution and least severe for the ethanediol. Two factors may be responsible for this ordering. First, fingering becomes more severe with increased mobility contrast. (The xanthan solution is the most viscous, while ethanediol is the least viscous of the three fluids.) Second, fingering is reported to be more severe for shear-thinning fluids than for Newtonian fluids.[26,30] (The xanthan solution is the most pseudoplastic of the fluids, while ethanediol is Newtonian.)

Field Verification

The theoretical analyses provided here and elsewhere[4,5,17] indicate that injection profiles usually are not expected to improve significantly in unfractured wells if gels are placed without zone isolation. Is field experience consistent with this conclusion? In Chap. 8 of Ref. 17, an analysis was performed with 43 pairs of injection profiles reported in the petroleum literature. For each pair, one profile was obtained before the gel treatment and another profile was obtained after the gel treatment. For 30% of the cases, the injection profile was improved noticeably after the gel treatment, while the profile was clearly not improved in 40% of the treatments. In the remaining cases, the profile changes were slight or ambiguous. Most of the available literature does not provide enough information to judge whether the wells were fractured before the gel treatment. Thus, the petroleum literature does not provide enough information to confirm or to contradict the theoretical predictions.[17] In view of the sporadic success of gel treatments,[1-3] identification of when zone isolation is needed during gel placement is a critical matter. Some well-designed field tests could help to resolve this issue.

Zone isolation can significantly improve the performance of gel treatments in some applications. These include unfractured injection wells with noncommunicating layers. Of course, cement squeezes can be equally effective in these applications. If zone isolation is not feasible, then our analyses raise doubts that gel treatments can be effective in unfractured injection wells. Gel treatments are more likely to improve sweep efficiency in wells where fractures are the source of the channeling problem. The search con-

tinues for properties that can be exploited to optimize gel placement (including pH dependence of gelation, gelation kinetics, and apparent rheology during and after gelation).[17]

Conclusions

1. For near-wellbore gel treatments in unfractured injection wells, diffusion and/or dispersion usually will not eliminate the need for zone isolation during gel placement.
2. During gel placement in parallel laboratory corefloods, diffusion and dispersion can cause one to conclude erroneously that zone isolation is not needed during gel placement in field projects.
3. For near-wellbore gel treatments in unfractured injection wells, a water postflush usually will not eliminate the need for zone isolation during gel placement.
4. If a viscous fluid is injected into a radial, multilayer system (with noncommunicating layers) and then followed by a water postflush, both theory and experiments indicate that viscous fingers usually will break through the viscous bank in the most-permeable layer first. At the time of this breakthrough, however, the fingers will have traversed most of the viscous bank in a less-permeable layer.

Nomenclature

D = apparent diffusion coefficient in porous media, in.^{2}/sec [cm^2/s]
D_o = molecular binary diffusion coefficient, in.^{2}/sec [cm^2/s]
F_r = resistance factor (brine mobility divided by mobility of the gelling agent)
F_{rr} = residual resistance factor (brine mobility before gel placement divided by brine mobility after gel placement)
F_μ = effective viscosity ratio for mixing zone (Eq. 6)
$F_{\mu p}$ = effective viscosity ratio for mixing zone (Eq. 9)
H = Koval heterogeneity factor
k_1 = permeability of most-permeable layer, md
k_2 = permeability of less-permeable layer, md
L = bank length, ft [m]
L_f = final bank length after dispersion, ft [m]
L_m = mixing-zone length, ft [m]
L_{pf} = length of postflush in absence of fingering, ft [m]
L_{pi} = distance gelling agent has propagated in linear core or from face of vertical fracture (into rock matrix) in Layer i, ft [m]
L_{pm} = maximum distance that gelling agent will propagate from fracture face in most-permeable core, ft [m]
L_{vf} = length of fingered zone in linear flow, ft [m]
Δp_{Di} = pressure drop between r_{pm} (or L_{pm}) and production well divided by pressure drop between injection well and r_{pm} (or L_{pm}) in Layer i
r_{fi} = final inner radius of viscous fluid after postflush, ft [m]
r_{fo} = final outer radius of viscous fluid after postflush, ft [m]
r_{pf} = radius of postflush in absence of fingering, ft [m]
r_{pi} = radius of penetration of gelling agent in Layer i, ft [m]
r_{pm} = maximum radius of penetration of gelling agent in most-permeable layer, ft [m]
r_{vf} = length of fingered zone in radial flow, ft [m]
r_w = wellbore radius, ft [m]
R = formation electrical resistivity
t = time, days
t_g = gelation time, days
α = dispersivity, ft [m]
ϕ_1 = porosity associated with aqueous phase in most-permeable layer
ϕ_2 = porosity associated with aqueous phase in less-permeable layer

Acknowledgments

This work was financially supported by the U.S. DOE, the New Mexico R&D Inst., Amoco Production Co., Conoco Inc., Elf Aquitaine, Marathon Oil Co., Oryx Energy, Oxy U.S.A., Phillips Petroleum Co., Shell Development Co., and Texaco Inc. Michael Carr performed the parallel beadpack floods, and his contribution is appreciated. I also appreciate the help of the staff of the New Mexico Petroleum Recovery Research Center in preparing and reviewing this paper.

References

1. Leonard, J.: "Increased Rate of EOR Brightens Outlook," *Oil & Gas J.* (April 14, 1986) 88–94.
2. Schurz, G. *et al.*: "Polymer Augmented Waterflooding and Control of Reservoir Heterogeneity," *Proc.*, Petroleum Technology Into the Second Century Symposium, Socorro, NM (Oct. 16–19, 1989) 263–75.
3. "Near-Wellbore Technology," Brochure 1024-87TL, Phillips Petroleum Co., Bartlesville, OK (1987).
4. Seright, R.S.: "Placement of Gels To Modify Injection Profiles," paper SPE 17332 presented at the 1988 SPE/DOE Enhanced Oil Recovery Symposium, Tulsa, April 17–20.
5. Seright, R.S.: "Effect of Rheology on Gel Placement," *SPERE* (May 1991) 212–18.
6. Zapata, V.J. and Lake, L.W.: "A Theoretical Analysis of Viscous Cross Flow," paper SPE 10111 presented at the 1981 SPE Annual Technical Conference and Exhibition, San Antonio, Oct. 5–7.
7. Zapata, V.J.: "A Theoretical Analysis of Viscous Crossflow," PhD dissertation, U. of Texas, Austin (1981).
8. Young, T.S., Willhite, G.P., and Green, D.W.: "Study of Intra-Molecular Crosslinking of Polyacrylamide in Cr(III)-Polyacrylamide Gelation by Size-Exclusion Chromatography, Low-Angle Laser Light Scattering, and Viscometry," *Water-Soluble Polymers for Petroleum Recovery*, G.A. Stahl and D.N. Schulz (eds.), Plenum Press, New York City (1988) 329–42.
9. Erdey-Gruz, T.: *Transport Phenomena in Aqueous Solutions*, John Wiley and Sons, New York City (1974) 151–63.
10. Southwick, J.G., Jamieson, A.M., and Blackwell, J.: "Conformation of Xanthan Dissolved in Aqueous Urea and Sodium Chloride Solutions," *Carbohydrate Research* (1982) **99**, 117–27.
11. Perkins, T.K. and Johnston, O.C.: "A Review of Diffusion and Dispersion in Porous Media," *SPEJ* (March 1963) 70–84; *Trans.*, AIME, **228**.
12. Prud'homme, R.K. and Uhl, J.T.: "Kinetics of Polymer/Metal-Ion Gelation," paper SPE 12640 presented at the 1984 SPE/DOE Enhanced Oil Recovery Symposium, Tulsa, April 15–18.
13. Southard, M.Z., Green, D.W., and Willhite, G.P.: "Kinetics of the Chromium (VI)/Thiourea Reaction in the Presence of Polyacrylamide," paper SPE 12715 presented at the 1984 SPE/DOE Enhanced Oil Recovery Symposium, Tulsa, April 15–18.
14. Arya, A. *et al.*: "Dispersion and Reservoir Heterogeneity," *SPERE* (Feb. 1988) 139–48.
15. Kolodziej, E.J.: "Transport Mechanisms of Xanthan Biopolymer Solutions in Porous Media," paper SPE 18090 presented at the 1988 SPE Annual Technical Conference and Exhibition, Houston, Oct. 2–5.
16. Heller, J.P.: "The Interpretation of Model Experiments for the Displacement of Fluids Through Porous Media," *AIChE J.* (1963) **9**, No. 4, 452–59.
17. Seright, R.S. and Martin, F.D.: "Fluid Diversion and Sweep Improvement With Chemical Gels in Oil Recovery Processes," first annual report, Contract No. DE-FG22-89BC14447, U.S. DOE (April 1991) 63–86.
18. Tang, D.H.E. and Peaceman, D.W.: "New Analytical and Numerical Solutions for the Radial Convection-Dispersion Problem," *SPERE* (Aug. 1987) 343–59.
19. Coats, K.H. and Smith, B.D.: "Dead-End Pore Volume and Dispersion in Porous Media," *SPEJ* (March 1964) 73–84; *Trans.*, AIME, **231**.
20. Perkins, T.K., Johnston, O.C., and Hoffman, R.N.: "Mechanics of Viscous Fingering in Miscible Systems," *SPEJ* (Dec. 1965) 301–17; *Trans.*, AIME, **234**.
21. Koval, E.J.: "A Method for Predicting the Performance of Unstable Miscible Displacement in Heterogeneous Media," *SPEJ* (June 1963) 145–54; *Trans.*, AIME, **228**.
22. Claridge, E.L.: "Prediction of Recovery in Unstable Miscible Flooding," *SPEJ* (April 1972) 143–55.
23. Claridge, E.L.: "Control of Viscous Fingering in Enhanced Oil Recovery Processes: Effect of Heterogeneities," paper SPE 7662 available from SPE, Richardson, TX.
24. Todd, M.R. and Longstaff, W.J.: "The Development, Testing, and Application of a Numerical Simulator for Predicting Miscible Flood Performance," *JPT* (July 1972) 874–82; *Trans.*, AIME, **253**.

Author

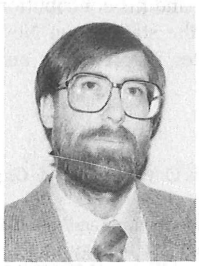

Randy S. Seright is senior engineer in charge of improved waterflooding and chemical flooding processes at the New Mexico Petroleum Recovery Research Center in Socorro. Previously, he worked for Exxon Production Research Co. He holds a PhD degree in chemical engineering from the U. of Wisconsin, Madison. Seright served on the program committee for the 1989 SPE Oilfield Chemistry Symposium; he is on the committee for the 1991 symposium and is a member of the Editorial Review Committee.

25. Stalkup, F.I.: *Miscible Displacement,* Monograph Series, SPE, Richardson, TX (1983) **8**, 39–44.
26. Stoneberger, M.W. and Claridge, E.L.: "Graded-Viscosity-Bank Design With Pseudoplastic Fluids," *SPERE* (Nov. 1988) 1221–32.
27. Clifford, P.J. and Sorbie, K.S.: "The Effects of Chemical Degradation on Polymer Flooding," paper SPE 13586 presented at the 1985 SPE Intl. Symposium on Oilfield and Geothermal Chemistry, Phoenix, April 9–11.
28. Clifford, P.J.: "Simulation of Small Chemical Slug Behavior in Heterogeneous Reservoirs," paper SPE 17399 presented at the 1988 SPE/DOE Enhanced Oil Recovery Symposium, Tulsa, April 17–20.
29. Sorbie, K.S. and Clifford, P.J.: "The Simulation of Polymer Flow in Heterogeneous Porous Media," *Water-Soluble Polymers for Petroleum Recovery,* G.A. Stahl and D.N. Schulz (eds.), Plenum Press, New York City (1988) 69–99.
30. Allen, E. and Boger, D.V.: "The Influence of Rheological Properties on Mobility Control in Polymer-Augmented Waterflooding," paper SPE 18097 presented at the 1988 SPE Annual Technical Conference and Exhibition, Houston, Oct. 2–5.

SI Metric Conversion Factors

ft	×	3.048*	E−01	= m
in.	×	2.54*	E+00	= cm
in.^{2}	×	6.451 6*	E+00	= cm^2
md	×	9.869 233	E−04	= μm^2

*Conversion factor is exact.

SPERE

Original SPE manuscript received for review March 8, 1990. Paper accepted for publication July 6, 1990. Revised manuscript received June 26, 1990. Paper (SPE 20127) first presented at the 1990 SPE Permian Basin and Gas Recovery Conference held in Midland, March 8–9.